Journal of Applied Microbiology

Journal of Applied Microbiology ISSN 1364-5072

ORIGINAL ARTICLE

Whole cell kinetics of ureolysis by *Sporosarcina pasteurii*

E.G. Lauchnor[1,2], D.M. Topp[1,3], A.E. Parker[1,4] and R. Gerlach[1,3]

1 Center for Biofilm Engineering, Montana State University, Bozeman, MT, USA
2 Department of Civil Engineering, Montana State University, Bozeman, MT, USA
3 Department of Chemical and Biological Engineering, Montana State University, Bozeman, MT, USA
4 Department of Mathematical Sciences, Montana State University, Bozeman, MT, USA

Keywords
ammonium inhibition, Michaelis–Menten model, microbial kinetics, pH inhibition, *Sporosarcina pasteurii*, ureolysis.

Correspondence
Ellen Lauchnor, Montana State University, 59717-3980, P.O. Box 173980, Room 366 EPS Bozeman, MT, USA.
E-mail: ellen.lauchnor@biofilm.montana.edu
and
Robin Gerlach, Montana State University, 59717-3980, P.O. Box 173980, Room 366 EPS Bozeman, MT, USA.
E-mail: robin_g@biofilm.montana.edu

2014/2359: received 17 November 2014, revised 10 February 2015 and accepted 26 February 2015

doi:10.1111/jam.12804

Abstract

Aims: Ureolysis drives microbially induced calcium carbonate precipitation (MICP). MICP models typically employ simplified urea hydrolysis kinetics that do not account for cell density, pH effect or product inhibition. Here, ureolysis rate studies with whole cells of *Sporosarcina pasteurii* aimed to determine the relationship between ureolysis rate and concentrations of (i) urea, (ii) cells, (iii) NH_4^+ and (iv) pH (H^+ activity).
Methods and Results: Batch ureolysis rate experiments were performed with suspended cells of *S. pasteurii* and one parameter was varied in each set of experiments. A Michaelis–Menten model for urea dependence was fitted to the rate data ($R^2 = 0{\cdot}95$) using a nonlinear mixed effects statistical model. The resulting half-saturation coefficient, K_m, was 305 mmol l^{-1} and maximum rate constant, V_{max}, was 200 mmol l^{-1} h^{-1}. However, a first-order model with $k_1 = 0{\cdot}35$ h^{-1} fit the data better ($R^2 = 0{\cdot}99$) for urea concentrations up to 330 mmol l^{-1}. Cell concentrations in the range tested (1×10^7–2×10^8 CFU ml^{-1}) were linearly correlated with ureolysis rate (cell dependent $V'_{max} = 6{\cdot}4 \times 10^{-9}$ mmol CFU^{-1} h^{-1}).
Conclusions: Neither pH (6–9) nor ammonium concentrations up to 0·19 mol l^{-1} had significant effects on the ureolysis rate and are not necessary in kinetic modelling of ureolysis. Thus, we conclude that first-order kinetics with respect to urea and cell concentrations are likely sufficient to describe urea hydrolysis rates at most relevant concentrations.
Significance and Impact of the Study: These results can be used in simulations of ureolysis driven processes such as microbially induced mineral precipitation and they verify that under the stated conditions, a simplified first-order rate for ureolysis can be employed. The study shows that the kinetic models developed for enzyme kinetics of urease do not apply to whole cells of *S. pasteurii*.

Introduction

Urea hydrolysis (ureolysis) is a microbial process that can promote the precipitation of carbonates such as calcium carbonate ($CaCO_3$) by producing dissolved inorganic carbon and increasing the saturation state of carbonate minerals (Mitchell *et al.* 2008; DeJong *et al.* 2010; van Paassen *et al.* 2010). The $CaCO_3$ can act as a biogenic cement in porous media and potentially plug small fractures where conventional cement cannot penetrate, which has led to interest in developing microbially induced calcium carbonate precipitation (MICP) as a cement alternative in some engineering applications (DeJong *et al.* 2010; Cunningham *et al.* 2013; Phillips *et al.* 2013). Potential applications of MICP include sequestering groundwater contaminants, such as radionuclides, in $CaCO_3$ (Fujita *et al.* 2010), soil stabilization and consolidation (De Muynck *et al.* 2010; DeJong *et al.* 2010), and plugging subsurface fractures near well bores to manipulate fluid transport (Cunningham *et al.* 2013; Cuthbert

et al. 2013). Ureolysis driven MICP provides a biologically driven process that requires a low-cost substrate (urea) and is highly effective in model organisms, such as *Sporosarcina pasteurii* (Stocks-Fischer *et al.* 1999; Phillips *et al.* 2013).

Ureolysis driven MICP involves a single enzyme-catalysed reaction, which can be easily modelled if the reaction kinetics are known (Mobley and Hausinger 1989; Krajewska 2009; Chahal *et al.* 2011; Burbank *et al.* 2012). Modelling studies have been utilized to make predictions and optimize ureolysis driven MICP for field applications (Zhang and Klapper 2010; Barkouki *et al.* 2011; Ebigbo *et al.* 2012). To create a model that accurately evaluates the potential for successful application of ureolytic MICP, a better understanding of the kinetic parameters for the microbially driven ureolysis reaction is needed.

Thus far, increasingly complex models of enzyme-based ureolysis kinetics have been developed (Fidaleo and Lavecchia 2003), which add to model uncertainty and may not apply to whole cell systems (Ebigbo *et al.* 2012). The ureolysis reaction is likely to exhibit Michaelis–Menten behaviour when whole cells are used as catalysts, though the kinetic parameters will differ from those determined for the enzyme due to the necessary transport of urea into the cell.

Ureolysis is catalysed by urease (urea amidohydrolase) and the overall equation is shown in Eqn (1). The production of NH_3 by ureolysis ultimately results in an increase in the pH of the system. Ureolysis also increases the dissolved inorganic carbon concentration of a system and in systems with carbonate alkalinity this increase in pH shifts the carbonate equilibrium towards CO_3^{2-}. Urease is a widespread enzyme in bacteria and is produced by some plants, such as soybean and jack bean (Krajewska 2009). MICP studies have mostly focused on the ureolytic soil bacterium *S. pasteurii* due to the high urease production and constitutive expression of the enzyme (Mobley *et al.* 1995; DeJong *et al.* 2010; Cunningham *et al.* 2013; Phillips *et al.* 2013).

$$CO(NH_2)_2 + 2H_2O \rightarrow 2NH_3 + H_2CO_3 \qquad (1)$$

Kinetic models of urea hydrolysis by jack bean urease have been developed which incorporate pH dependence, temperature dependence and NH_4^+ concentration (Moynihan *et al.* 1989; Qin and Cabral 1994; Fidaleo and Lavecchia 2003; Krajewska *et al.* 2012). The Michaelis–Menten model has been widely used in such studies, which is described by two parameters: the maximum rate constant which represents the highest reaction rate possible for the enzyme (V_{max}), and the half-saturation coefficient (K_m), which is the concentration at which the reaction proceeds at half the maximum rate (Cornish-Bowden 2004).

In addition, urease produced by the bacterium *S. pasteurii* has been extracted and subjected to kinetic studies, including Michaelis–Menten based models (Krajewska 2009). *Sporosarcina pasteurii* cell extract urease was found to have a maximum activity at pH 8·0 with a strong pH dependence on the enzyme activity (Stocks-Fischer *et al.* 1999). Bachmeier *et al.* (2002) determined that immobilizing the enzyme increases the apparent K_m and decreases V_{max} due to mass transfer limitations (Bachmeier *et al.* 2002).

Many engineering applications of ureolytic MICP focus on cell- or biofilm-based systems, which may differ from the observed enzyme kinetics. Whole cell studies of MICP have typically assumed zero- or first-order ureolysis rates with respect to substrate concentration (Ferris *et al.* 2003; Okwadha and Li 2010; Tobler *et al.* 2011; Cuthbert *et al.* 2012). Additionally, studies have not incorporated the influence of cell concentration on ureolysis due to limitations of measuring cell viability during MICP (Kantzas *et al.* 1992; Ferris *et al.* 2003; Dupraz *et al.* 2009). However, the positive correlation between cell concentration (inoculum size) and ureolysis rate has been recognized in recent studies (Okwadha and Li 2010; Tobler *et al.* 2011; Cuthbert *et al.* 2012). One recent study has evaluated ureolysis kinetics during batch growth of *S. pasteurii* (Connolly *et al.* 2013). Here, the ureolysis reaction is isolated from growth by short term experiments (1 h) that limit growth and product accumulation.

In this study we use suspended cell experiments to investigate the influence of four parameters on the kinetics of urea hydrolysis by whole cell cultures of the bacterium *S. pasteurii* (ATCC 11859): (i) urea concentration, (ii) cell density, (iii) NH_4^+ concentration and (iv) pH. The results of these investigations provide insight into the appropriateness of different kinetic expressions that can be incorporated into reactive transport model simulations, rate predictions and the optimization of ureolytic MICP applications.

Materials and methods

Growth and kinetic media

Growth medium for overnight cultures of *S. pasteurii* consisted of 37 g l^{-1} Brain Heart Infusion (Becton Dickinson, Franklin Lakes, NJ) and 20 g l^{-1} urea (Fisher Scientific, Inc., Pittsburgh, PA) in deionized water, and was sterilized by autoclaving at 121°C for 20 min. The medium used for ureolysis batch experiments contained 3 g l^{-1} Difco nutrient broth (BD, Franklin Lakes, NJ), 0–10 g l^{-1} ammonium chloride (Fisher Scientific, Pittsburg, PA) and 0·05–45 g l^{-1} urea (Fisher Scientific, Pittsburg, PA) in deionized water. The medium was adjusted to pH

6·0 and filter sterilized using SteriTop 0·2 μm bottle top filters (Nalgene, Rochester, NY). The standard ureolysis medium consisted of 330 mmol l^{-1} urea (20 g l^{-1}), 187 mmol l^{-1} NH_4Cl (10 g l^{-1}) and 3 g l^{-1} nutrient broth, which was used as a control case for each experiment to demonstrate no significant variations in ureolytic activity between *S. pasteurii* cultivated for the different experiments in this work. This medium recipe is used by our group in laboratory and field scale experiments, thus the growth and ureolysis behaviour of *S. pasteurii* is well known under these conditions, making it an ideal positive control for the studies.

Culture preparation

A frozen stock (1 ml) of *S. pasteurii* (ATCC 11859) was added to 100 ml of growth medium. The culture was shaken for 24 h at 150 rev min^{-1} and 30°C and 1 ml was transferred to 100 ml of fresh growth medium and incubated under the same conditions for 13–16 h, at the end of which cells were in late exponential growth phase. For each batch experiment, 100 ml of the culture was centrifuged at a relative centrifugal force of 2964 ***g*** for 10 min. The cell pellet was resuspended in 5 ml fresh growth medium. Centrifugation and resuspension were repeated three times, after which an aliquot of the concentrated cell suspension was added to 100 ml of medium in each batch reactor. For all batch experiments except the variable cell concentration studies, the final cell density in suspension had an average OD_{600} of 0·1 (±12%) on a Synergy HT reader (Biotek Instruments, Inc., Winooski, VT) in a 96-well plate with 100 μl per well.

Batch kinetic experiments

Batch reactors for the kinetic rate experiments consisted of sterile 250 ml Wheaton bottles with septa caps, containing 100 ml of liquid medium. The 150 ml headspace remaining in the reactors provided adequate oxygen for the 1 h long experiments. After inoculation with 1 ml of concentrated culture, bottles were placed in a shaker incubator at 30°C and 150 rev min^{-1}. Samples were taken at 10 or 15 min intervals for 2 h to monitor urea, pH, NH_4^+ and OD_{600}. The total volume of liquid sampled from the batch reactors amounted to 15% or less of the liquid volume in the reactors.

The reactors were sampled by inserting a needle through the septa and withdrawing 1·5 ml of liquid sample into a syringe. An aliquot of the liquid sample (0·5 ml) was filtered through syringe filters with 0·2 μm pore size and the samples were stored in 1·5 ml microcentrifuge tubes at 4°C until further analyses. The remainder of the unfiltered liquid sample (1 ml) was used to measure pH and OD_{600}.

The control variables NH_4^+, pH, cell density and urea concentration were evaluated in the batch experiments by varying one parameter in the initial conditions for each set of experiments. Table 1 shows the experimental conditions used to investigate each parameter. In the pH experiments, buffers at a total concentration of 100 mmol l^{-1} were as follows: pH 5: citric acid/sodium citrate, pH 6: NaH_2PO_4/Na_2HPO_4, pH 7: TRIS-HCl/TRIS base, pH 8: HEPES buffer, pH 9: CHES buffer, pH 10: $NaHCO_3/Na_2CO_3$. In preliminary tests, cells grew successfully overnight in growth medium containing each buffer solution, indicating that the buffers were not toxic to the cells under the growth conditions.

Analytical methods

Urea was measured using a method consisting of a derivatization reaction and detection via HPLC as described previously (Lauchnor *et al.* 2013). Colony forming units in the inoculum were determined by performing serial dilution and drop plating to verify the initial bacterial concentration (Herigstad *et al.* 2001).

Kinetic models

The initial ureolysis rate for the first hour of each experiment was calculated from the slope of urea concentration over time. The concentration and initial rate for each test was used to fit the data to several kinetic models. An assumption involved in the initial rate method is that a linear rate can be determined at early time points (first hour) before concentrations in the solution have changed significantly (Cornish-Bowden 2004). Thus, a single rate corresponding to the initial urea concentration is determined for each batch experiment. The rate analysis was performed for triplicate flasks at each condition, and the averages and standard deviations of triplicates were calculated from the individual rates.

$$R_u = \frac{\Delta[\text{urea}]}{\Delta t} \tag{2}$$

The initial rate (R_u) in mol l^{-1} h^{-1} was estimated for each experiment by calculating the slope of [urea] vs time for the first hour (Eqn (2)). Then, for each rate test the urea concentration at initial time ($t = 0$) was correlated with the rate calculated for that experiment, resulting in a pair of values ($[\text{urea}_i]$, $R_{u,i}$) for each experiment (Table S1). First order and Michaelis–Menten kinetic models were investigated to assess the dependence of ureolysis rate on substrate (urea) concentration.

In Eqn (3) describing the first-order ureolysis rate in mol l^{-1} h^{-1} (R_u), k_1 is the first-order rate constant with

Table 1 Summary of experimental conditions for each parameter of interest

Experiment	Parameter	NH_4Cl (mmol l^{-1})	Urea (mmol l^{-1})	pH	OD_{600}
1	Substrate (urea)	187	1–722	6·0–9·3*	0·025
2	Cell concentration	187	333	6·0–9·3*	0·025, 0·075, 0·10, 0·15
3	Product (NH_4^+)	6, 23, 147	54	6·0–9·3*	0·025
4	pH (Buffered)	187	54	5, 6, 7, 8, 9, 10	0·025

*Unbuffered medium, see Fig. 1b,d. Initial pH was 6·0, final pH was 9·3.

units of h^{-1} and [urea] is the urea concentration in mol l^{-1}.

$$R_u = -k_1[\text{urea}] \quad (3)$$

The Michaelis–Menten model is a commonly used kinetic model describing enzyme-catalysed reactions. Equation (4) was used as the Michaelis–Menten-based equation for the ureolysis reaction in terms of [urea]:

$$R_u = -\left(\frac{V_{\max}[\text{urea}]}{K_m + [\text{urea}]}\right) \quad (4)$$

The Michaelis–Menten term on the right side of Eqn (4) is negative as it represents consumption of urea. The constant K_m is the half-saturation coefficient with units of molar urea concentration, and $V_{\max}$ is the maximum rate of reaction with units of urea concentration per time. As in the first-order model, the initial rate method was used, where [urea] is the initial urea concentration from each batch test and R_u is the corresponding rate.

Statistical methods of parameter estimation

Initial rate calculations were performed for each individual reactor before averaging. The individual rates for each reactor were used for the parameter estimation, although the data are condensed into the averages and standard deviations of the triplicates in Table 2. The complete data set is shown in the Supplemental Information (Table S1). The experimental data ($[\text{urea}_i]$, $R_{u,i}$) was used to fit k_1 in Eqn (3) using a linear regression.

Two different statistical models were used for parameter estimation in Eqn (4); nonlinear least-squares (nls) and nonlinear mixed effects (*nlme*). A nonlinear least-square (nls) method was employed to optimize fitting of Michaelis–Menten parameters to the data. In this method, the combined residual sum of squared error was minimized between the model and experimental rates to determine the most likely estimates for the kinetic coefficients. A second method for parameter estimation, nonlinear mixed effects (*nlme*), was also used to estimate the optimized values of Michaelis–Menten parameters while incorporating random effects such as differences in experimental date. The *nlme* model first determined whether random effects were influential in fitting the model to the experimental data, which can occur as a result of running experiments with bacterial cultures grown on different days. If random effects were influential, then updated estimates of the kinetic coefficients were provided.

Table 2 Averages and standard deviations of triplicate ureolysis rate batch experiments with varying urea concentrations. Initial urea values were measured before the addition of bacteria. Reactors in the same experimental group were tested on the same day with the same bacterial culture as inoculum

Experimental group	Initial urea, $[\text{urea}_i]$ mmol l^{-1}	Initial rate, $R_{u,i}$ mmol l^{-1} h^{-1}	Standard deviation of rate, mmol l^{-1} h^{-1}*
1	722	129	16
2	542	129	16
1	423	133	9
1	314	116	14
3	319	114	7
2	266	86	10
3	179	53	1
3	54	16	3
3	18	6·8	2·1
3	7·5	1·4	0·1
2	3·8	1·9	0·4
2	1·1	0·6	0·2

*Standard deviations of rates were calculated from individual rates of triplicate batch experiments.

The solver function in Microsoft Excel, Office 2010 (Microsoft Corporation, Redmond, WA) and MATLAB ver. R2013a (MathWorks, Inc., Natick, MA) were used independently for parameter estimation using the nls method. The two programs generated the same optimized parameters estimated by the nonlinear least-square approach. The R package *nlme* (Team 2012) was used to conduct parameter estimation on the data set by nonlinear mixed effects optimization (Pinheiro and Bates 2000; Pinheiro *et al.* 2012).

Results

Urea dependent kinetics

The initial ureolysis rate was determined at varying urea concentrations in the batch reactors while maintaining

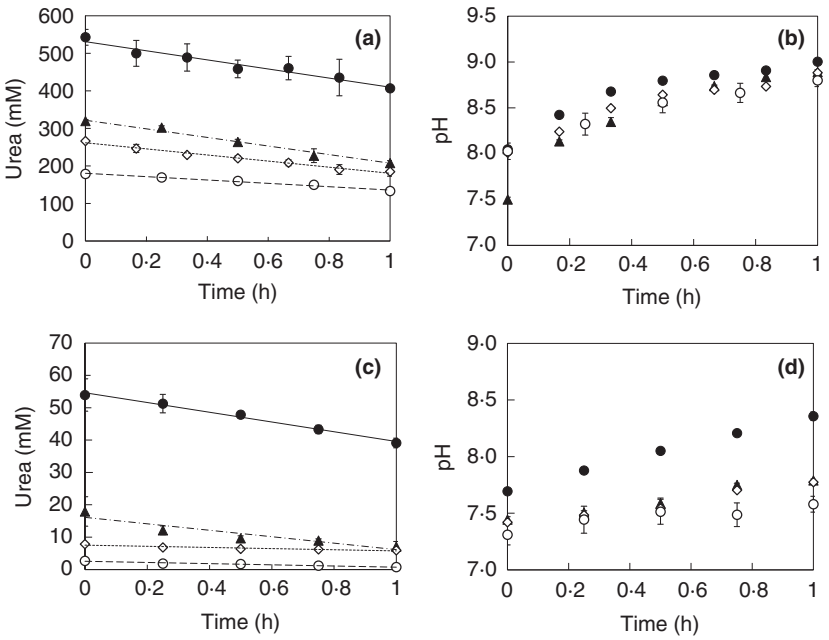

Figure 1 Urea (a, c) and pH (b, d) over time in batch experiments with varying concentrations of initial urea. (a) and (b) high concentration range in mmol l^{-1} urea: (○) 179, (◊) 266, (▲) 314, (●) 542, (c) and (d) low concentration range in mmol l^{-1} urea: (○) 3·8, (◊) 7·5, (▲) 18, (●) 54. In all batch experiments, biomass concentration was $3{\cdot}4 \pm 0{\cdot}4{*}10^7$ CFU ml^{-1}. Error bars show standard deviations of experimental triplicates.

relatively constant biomass concentration over 1 h. Results of urea and pH analysis with initial urea concentrations between 179 and 542 mmol l^{-1} are shown Fig. 1a,b. In all of these experiments, the pH approached 9·0 over the first hour due to production of NH_3 and consumption of protons during acid/base equilibration of the NH_4^+/NH_3 buffer system. The cell concentrations were measured in all experiments and CFU ml^{-1} only varied 30% between all batch reactors and over the duration of the experiments.

Figure 1c,d show urea concentration and pH, respectively, for batch experiments performed with initial urea concentrations between 3·8 and 54 mmol l^{-1}. In the presence of low initial urea concentrations (Fig. 1d), the pH did not increase rapidly due to slower production of NH_3, and thus the pH was still well below 9·0 after 1 h. In these systems, due to the absence of calcium and inability for $CaCO_3$ precipitation, the extent of ureolysis correlates directly to the pH increase, as the production of NH_4^+ is the most significant driving force for pH change in the system.

Linear regression lines shown in Fig. 1a,c correspond to the calculated linear slope values used for initial rate analysis. The linearly changing urea concentrations in Fig. 1 indicate that the initial rate method approach (Cornish-Bowden 2004) was valid for the 1 h duration of these experiments. Table 2 summarizes the urea concentrations and calculated rates from the experiments in Fig. 1, which were used as inputs for kinetic model analysis.

Increasing ureolysis rates correlate with higher urea concentrations up to 314 mmol l^{-1}, above which the

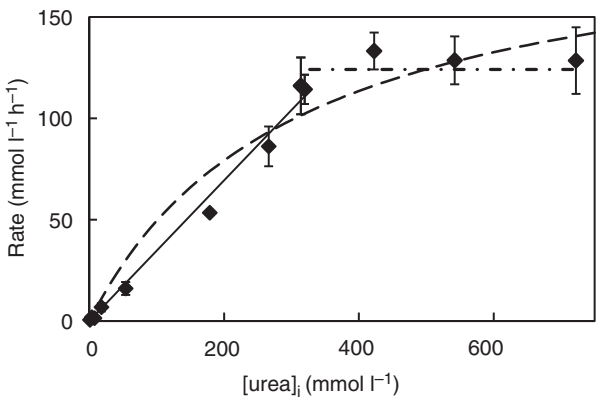

Figure 2 Summary of batch experimental results with varying urea concentrations. Symbols (♦) indicate experimental results with error bars representing standard deviation of triplicate samples. The data is shown as the average of triplicate reactors, although the individual data points in Table 2 were used for parameter estimation. The model lines indicate the Michaelis–Menten model (Eqn 2) (long dash), first-order model up to 330 mmol l^{-1} urea (solid line), and zero-order model above 330 mmol l^{-1} (dash-dot).

ureolysis rate was relatively constant (Fig. 2). The nonlinear least-square estimates for the parameters for the Michaelis–Menten model in Eqn (4) were $V_{max} = 216$ mmol l^{-1} h^{-1} with a 95% confidence interval (CI) = [166, 266] and $K_m = 359$ mmol l^{-1} with a 95% CI = [184, 534] ($R^2 = 0{\cdot}95$).

The nonlinear mixed effects model was used to account for a random effect due to different cell culture growth or other changes between the different experi-

ments. A significant random effect due to K_m was identified among the different experimental dates. Thus, slight differences existed between the experimental dates and most of the uncertainty in the model was due to uncertainty in estimation of K_m. This resulted in smaller predicted values for the kinetic parameters: V_{max} = 200 mmol l^{-1} h^{-1} and K_m = 305 mmol l^{-1}. The mixed effects model also predicted a 95% CI for V_{max} of [153, 247] mmol l^{-1} h^{-1} and 95% CI for K_m of [139, 471] mmol l^{-1}. With either statistical method, a clear trend in residuals is present between the model and experimental data (Figure S1), indicating that the form of the Michaelis–Menten model in Eqn (4) does not entirely describe the kinetics of the ureolysis reaction.

The ureolysis rates at different urea concentrations were also fitted to a first-order relationship using linear regression, as in Eqn (3). If the entire concentration range is taken into account, a first-order approximation of ureolysis rate indicates a trend in residuals and an R^2 = 0·22. The first-order rate constant was fitted to the urea concentration range 1·1–319 mmol l^{-1}, resulting in a first-order rate constant of k_1 = 0·35 h^{-1} with a 95% CI of 0·02 h^{-1} and R^2 = 0·98 (Fig. 2). This indicated that ureolysis rate can be approximated as first order with respect to urea concentration, up to approx. 330 mol l^{-1} for *S. pasteurii*. However, in an effort to make the Michaelis–Menten model more accurate, the potential impacts of cell concentration, NH_4^+ and pH are evaluated in the following sections.

Sensitivity assessment

The sensitivity of the optimized values of V_{max} and K_m was assessed by varying each parameter independently 10 and 25% above and below the optimized value, while keeping the other parameter constant (Fig. 3). With the exception of the data point at 54 mmol l^{-1}, the variability in experimental results is within the range of the sensitivity analysis when V_{max} is increased or decreased by 25%. The R^2 values for rate models in the sensitivity analysis remained above 0·90, even when K_m or V_{max} deviated up to 25% from the optimized values (Fig. 3). This suggests that the model's fit to the data does not have a high degree of sensitivity to small changes in the optimized values for the parameters. The Michaelis–Menten model was the only model examined here that could be applied to the complete range of substrate concentrations (Fig. 2). Thus, this rate model was used for the remaining comparisons with pH, cell concentration and $[NH_4^+]$.

A sensitivity analysis was performed for the optimized values of V_{max} and K_m to determine the maximum sensitivity of the model fit. The model was shown to be most sensitive to changes in the parameters that satisfy $4*V_{max}-K_m$ (SI, Figure S3). This indicates that the model is impacted more by changes in V_{max} than K_m, which is supported by the results shown in Fig. 3 and also by the observation that most of the variability in the model is due to K_m uncertainty. Thus, it appears to be more important to accurately determine the maximum rate in the Michaelis–Menten model than the half-saturation coefficient.

Influence of bacterial cell concentration

Batch experiments at a single urea concentration (330 mmol l^{-1}) were performed with a range of cell concentrations, from 1×10^7–2×10^8 CFU ml^{-1} (Fig. 4). Optical density, or absorbance, is linearly proportional to the cell concentration in a solution according to the Beer-Lambert Law (Parks 2009). Therefore, Fig. 4 shows that ureolysis rate is linearly proportional to cell concentration within the range of cell concentrations utilized here. Likewise, other studies have found a positive correlation between cell density and ureolysis rate by *S. pasteurii* (Okwadha and Li 2010; Tobler *et al.* 2011). The data presented here clearly indicate a linear relationship between the apparent ureolysis rate and cell concentration, indicating that such a correlation can be included in a kinetic model of ureolysis within the cell concentration range evaluated here.

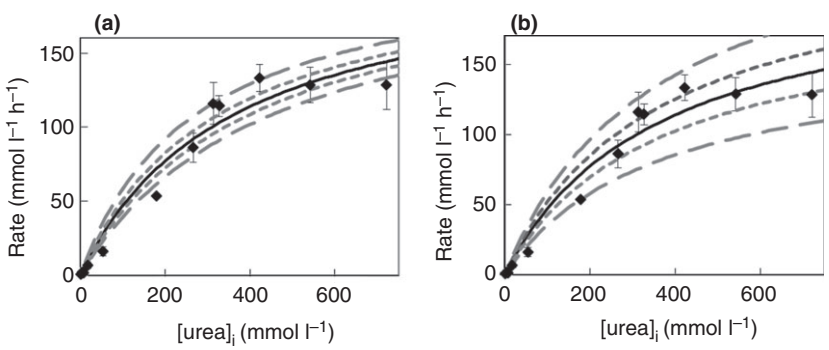

Figure 3 Sensitivity analysis of Michaelis–Menten parameters (a) K_m and (b) V_{max}. Black solid lines indicate the optimized model fit to the data (♦). Short dashed lines are the result of varying the parameter by ±10%, long dashed lines are the result of varying the parameter by ±25%. Error bars on the data points represent the standard deviation of triplicate reactors.

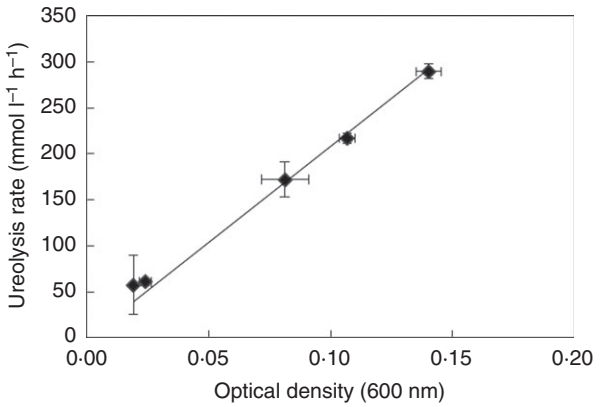

Figure 4 The linear relationship between optical density and ureolysis rate is an indication that the rate is directly proportional to the cell concentration. Error bars are the standard deviations of triplicate batch reactors.

In the urea dependent batch experiments, the inoculum was designed to yield the same initial cell density of $3{\cdot}4 \pm 0{\cdot}4 \times 10^7$ CFU ml^{-1} ($OD_{600} = 0{\cdot}026 \pm 0{\cdot}004$) in all experiments and the cell concentration increased due to growth by a maximum of only 30%. A biomass-normalized Michaelis–Menten model (Eqn (5)) was fitted to the data by dividing the ureolysis rate by the biomass concentration in each flask. The cell concentration [X] is considered a surrogate measurement for urease enzyme concentration. In *S. pasteurii* the urease enzyme is constitutively produced; thus the concentration of cells is assumed to be proportional to the enzyme concentration (Mobley *et al.* 1995).

$$\frac{\mathrm{d[urea]}}{\mathrm{d}t} = [X]\left(\frac{V'_{\max}[\mathrm{urea}]}{K'_m + [\mathrm{urea}]}\right) \qquad (5)$$

Equation (5) incorporates the assumption that the biomass concentration $[X]$ is linearly correlated with ureolysis rate, indicating that an increase in biomass should correspond to an increase in ureolysis rate. This assumption was based on the low range of bacterial cell concentrations that were used in the batch rate experiments, whereas in the case of high density biomass, such as in a biofilm, the assumption may not be valid. Cell concentration, $[X]$, was expressed as optical density at 600 nm (OD_{600}) because absorbance based measurements have a positive linear correlation with colony forming units of *S. pasteurii* (active biomass) (Parks 2009).

The nonlinear mixed effects model was used to estimate the parameters K'_m and $V'_{\max}$ in Eqn (5), using biomass-normalized ureolysis rate data. The result of parameter fitting resulted in a $V'_{\max}$ of $6{\cdot}4 \times 10^{-9}$ mmol urea CFU^{-1} h^{-1} and K'_m of 355 mmol l^{-1} and did not improve the R^2 value for the Michaelis–Menten model, which was 0·947 (Figure S2). Presumably, this was due to the fact that only small differences in cell concentration (30%) were observed.

Influence of ammonium concentration

NH_4^+ inhibition was evaluated by batch tests with varying initial NH_4Cl concentrations (Fig. 5a). In these experiments, 83 mmol l^{-1} urea (5 g l^{-1}) were used instead of 330 mmol l^{-1} to reduce the change in NH_4^+ concentration over the 1 h long experiments. The highest initial NH_4^+ concentration tested was 147 mmol l^{-1} as NH_4Cl, which resulted in a molar ratio of 1 mol urea:2 mol NH_4^+. A parallel control test with standard ureolysis medium containing 330 mmol l^{-1} urea resulted in a urea hydrolysis rate of 114 mmol l^{-1} h^{-1}, which verified that bacterial activity was consistent with the previously conducted 330 mmol l^{-1} experiments (Table 2).

Ureolysis rates were compared between the batch experiments performed without NH_4^+ and the three initial NH_4Cl concentrations of 147, 23 and 6 mmol l^{-1} (Fig. 5a). In all experiments, the initial pH of 6·3 increased to 7·5 after 1 h due to ureolysis. The ureolysis rate was not significantly different between the four cases (one-way ANOVA, P-value = 0·6). Therefore, in the concentration range of 0–147 mmol l^{-1} NH_4^+, the presence of NH_4^+ had no significant effect on the ureolysis rate. The average initial rate was 18 mmol l^{-1} h^{-1}

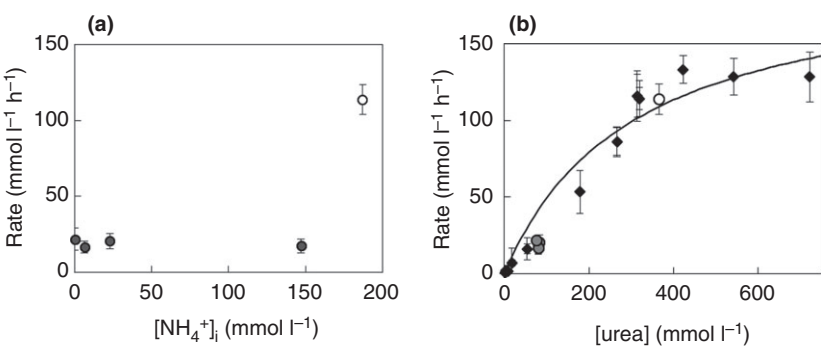

Figure 5 Comparison of ureolysis rates in the presence of different ammonium concentrations. (a) Ureolysis rates vs. [NH_4^+] with 5 g l^{-1} urea (●) and a control with 20 g l^{-1} urea (○). (b) Urea hydrolysis rates from experiments shown in part (a) (○) added to data shown in Figure 2 (♦). The Michaelis–Menten rate model fitted to the entire data set (line). Error bars are standard deviations of triplicate batch reactors.

(SD = 4 mmol l^{-1} h^{-1}) over the range of tested NH_4^+ concentrations.

Inhibition of ureolysis by NH_4^+ or NH_3 has been incorporated into previous models by addition of a noncompetitive product inhibition term to the Michaelis–Menten model, as shown in Eqn (6) (Qin and Cabral 1994; Fidaleo and Lavecchia 2003).

$$\frac{d[\text{urea}]}{dt} = [X]\left(\frac{V_{\max}[\text{urea}]}{(K_m + [\text{urea}])\left(1 + \frac{[NH_4^+]}{K_p}\right)}\right) \quad (6)$$

The results of experiments with varying NH_4Cl concentration aligned well with the rates from the original experiments with 187 mmol l^{-1} NH_4Cl and similar urea concentrations, as indicated by the proximity to the Michaelis–Menten curve (Fig. 5b). Therefore, an ammonium inhibition term does not appear to be required for kinetic models describing ureolysis. Thus, a determination of K_p is likely not needed since NH_4^+ does not inhibit ureolysis in the concentration range of NH_4^+ that might be produced during MICP applications (Phillips *et al.* 2013).

Influence of pH

Qualitative comparison of ureolysis rates over the pH range of 5–10 indicates a slight dependence on pH with the highest ureolysis rate near pH 9 (Fig. 6). The unbuffered controls exhibited slightly higher ureolysis rates than the pH buffered tests, which may indicate a minor effect of the buffer chemicals on enzyme activity. Based on multiple *t*-tests comparing the ureolysis rates at different pH values, the only statistically significant differences ($P < 0{\cdot}05$) existed between the rates at pH 9 and 10, and the rates at pH 5 and 9.

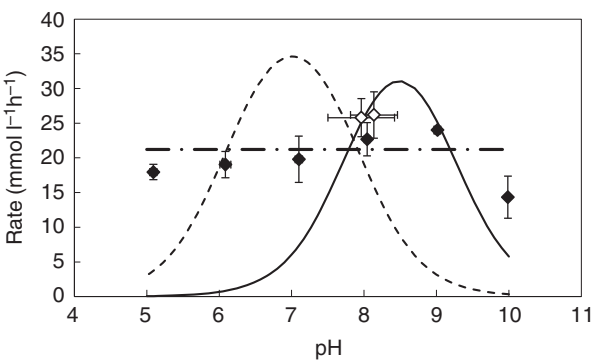

Figure 6 Ureolysis rates at different pH values with 83 mmol l^{-1} urea. Experimental results for buffered experiments at pH 5–10 (♦) and unbuffered controls (◊). Horizontal error bars are ranges of pH values for triplicate batch reactors. Vertical error bars are the standard deviations of ureolysis rates and are smaller than the markers if not visible. The model with fitted K_{es1} and K_{es2} according to equation 9 (solid line) is compared to the model using the values of $K_{es,1}$ and $K_{es,2}$ from Fidaleo and Lavecchia (2003) (dashed line). The horizontal line (dash-dot) indicates the average ureolysis rate of the experiments.

As noted above, a pH increase occurred during the experiments, with the greatest pH increase observed with 330 mmol l^{-1} initial urea or more (Fig. 1b,d). Previous studies of urease enzyme kinetics concluded that ureolysis is pH dependent (Moynihan *et al.* 1989; Qin and Cabral 1994; Ciurli *et al.* 1996; Fidaleo and Lavecchia 2003) and can be described using the model shown in Eqn (7):

$$\frac{d[\text{urea}]}{dt} = \left(\frac{V_{\max}[\text{urea}]}{(K_m + [\text{urea}])\left(1 + \frac{\{H^+\}}{K_{es,1}} + \frac{K_{es,2}}{\{H^+\}}\right)}\right) \quad (7)$$

The parameters $K_{es,1}$ and $K_{es,2}$ are acid-base equilibrium constants for protonation and deprotonation of the enzyme respectively. Cell concentration is not included here, as the experiments here were conducted at a single cell concentration. This kinetic model results from allowing urease to become protonated or deprotonated, which in turn impacts the activity of the enzyme (Fidaleo and Lavecchia 2003). For *S. pasteurii* urease, the optimal pH has been shown to be pH 8 under both suspended and immobilized conditions (Ciurli *et al.* 1996). Ciurli and others demonstrated that both fixed and free *S. pasteurii* urease would lose 80% of its ureolytic activity due to a pH increase above 9·0 or a decrease below pH 6·0.

Ureolysis rate models based on Eqn (7) are shown in Fig. 6. The model using the $K_{es,1}$ and $K_{es,2}$ parameter values determined by Fidaleo and Lavecchia (2003) ($7{\cdot}6*10^{-7}$ mol l^{-1} for $K_{es,1}$ and $1{\cdot}3*10^{-8}$ mol l^{-1} for $K_{es,2}$) does not provide a good fit to the data. An attempt to fit $K_{es,1}$ and $K_{es,2}$ in Eqn (7) by nonlinear least squares using the data in Fig. 6 and values of $V_{\max}$ (200 mmol l^{-1} h^{-1}) and K_m (305 mmol l^{-1}) was also unsuccessful (Fig. 6, solid line). These values for $V_{\max}$ and K_m were used because they were fitted using a range of urea concentrations, whereas the pH dependent experiments were performed with a single urea concentration and the data set in Fig. 6 was not sufficient to refit $V_{\max}$ and K_m.

The fitted values of $K_{es,1}$ and $K_{es,2}$ were both higher than those reported by Fidaleo and Lavecchia for jack bean urease (Fidaleo and Lavecchia 2003). The fitted values of $K_{es,1}$ and $K_{es,2}$ were $1{\cdot}6*10^{-8}$ mol l^{-1} and $6{\cdot}6*10^{-10}$ mol l^{-1}, respectively, however the rate model still did not correspond to the data.

The average rate for the pH buffered experiments is shown as a horizontal line in Fig. 6. The sum of squared error between the average rate and the data points was almost an order of magnitude smaller than the pH dependent model fit. This indicates that within the pH

range tested, the pH does not significantly influence the ureolysis rate by whole cell suspensions of *S. pasteurii*.

Discussion

In this work, the effects of urea (substrate) concentration and cell concentration were significant in the kinetic model, although NH_4^+ and pH did not have a significant impact on ureolysis rate. As seen in previous studies, the rate of ureolysis by *S. pasteurii* is dependent on urea concentration. A Michaelis–Menten model with respect to urea concentration was fitted to the entire concentration range of the batch data (1–720 mmol l^{-1}), although a first-order rate model was the best fit for urea concentrations in the range below 330 mmol l^{-1}. It is worth noting that urea concentrations used in many MICP applications and experiments are usually below 330 mmol l^{-1} urea (Phillips *et al.* 2013). This indicates that a first-order ureolysis rate model might be suitable for most real world MICP applications.

The K_m value of 305 mmol l^{-1} was determined by *nlme* for the Michaelis–Menten ureolysis model. Other studies have reported both higher and lower values for whole cell ureolysis by *S. pasteurii* (Kantzas *et al.* 1992; Connolly *et al.* 2013; Mahanty *et al.* 2014). Connolly *et al.* (2013) determined a lower K_m of 67 mmol l^{-1} in experiments during growth of biomass over 30 h, which may have resulted in uncertainty of the ureolysis rates. Mahanty and others determined a similar value to Connolly *et al.* of K_m = 44·1 mmol l^{-1} in a growth dependent study of *S. pasteurii* (Mahanty *et al.* 2014). Kantzas *et al.* performed a whole cell study with *S. pasteurii* and measured a K_m of 722·6 mmol l^{-1} (43 g l^{-1}), twice the value determined in the present study.

The affinity of urease in the whole cell study is lower than that of the extracted enzyme, indicated by the higher K_m value of whole cells (305 mmol l^{-1}) compared to purified enzyme K_m (17 mmol l^{-1}) (Bachmeier *et al.* 2002) or cell extract urease (26·2 mmol l^{-1} at pH 7·7) (Stocks-Fischer *et al.* 1999). This result is expected, as the affinity of urease inside a cell can be considered a lumped parameter that accounts for transport of the substrate into the cell in addition to the enzyme affinity. It has been shown that *S. pasteurii* is not likely to have an active transport mechanism for urea uptake into the cell (Jahns *et al.* 1988). Thus, urea uptake in *S. pasteurii* is dependent upon diffusion across the membrane driven by a concentration gradient.

The nonlinear mixed effects model determined that there was a small but significant random effect on ureolysis rates due to experiment-to-experiment sources (such as variation in the cell cultures grown on different days), and that variability between experiments influenced the fit of the Michaelis–Menten model to the data. However, the confidence intervals for the parameter estimates were large enough that according to the 95% confidence interval, the estimates made by nls and *nlme* were not significantly different. Additionally, the sensitivity analysis performed (Fig. 3) suggests that the model's fit to the data does not have a high degree of sensitivity to small changes in the optimized values for the parameters.

The first-order constant for ureolysis of 0·35 h^{-1} (8·4 day^{-1}) is higher than other published 1st order ureolysis rate constants for *S. pasteurii*. The k_{urea} values determined by Tobler and others were 0·044–0·10 h^{-1} (1·06–2·45 day^{-1}) for similar cell densities (Tobler *et al.* 2011), and Okwadha and Li determined k_{urea} values of 0·33–0·35 h^{-1} (0·80–0·85 day^{-1}) for higher cell concentrations (7–8 $\times$ 10^7 CFU ml^{-1}) and varying urea concentrations (Okwadha and Li 2010). These lower rate constants could be largely due to the presence of calcium in the other studies, resulting in precipitation of $CaCO_3$ on cells and potentially cell inactivation. For this reason, we did not supply calcium in order to obtain uninhibited ureolysis rate constants, and additional studies are necessary to quantify the bacterial deactivation by $CaCO_3$ precipitation.

Above the threshold concentration of 319 mmol l^{-1} urea (approx. 20 g l^{-1}), a zero-order approximation can be used for ureolysis by suspended cultures at a cell density of approx. 3·4*10^7 CFU ml^{-1}. However, based on the zero-order approximation at high urea concentrations the maximum ureolysis rate is 124 mmol l^{-1} h^{-1} (standard deviation 13 mmol l^{-1} h^{-1}), which is much lower than the Michaelis–Menten V_{max} value of 216 mmol l^{-1} h^{-1}. The residuals present in the Michaelis–Menten model follow a trend (Figure S1), suggesting that the model equation does not completely describe the relationship between urea concentration and ureolysis rate. However, the Michaels-Menten model is preferred over the first-order relationship when evaluating ureolysis over the entire concentration range in Fig. 2.

The cell concentration studies indicate that the inclusion of the biomass term [X] in Eqn (5) is necessary to fully describe the ureolysis rate with variable cell concentrations. In the cell concentration range of 1 $\times$ 10^7–2 $\times$ 10^8 CFU ml^{-1}, ureolysis was linearly dependent upon cell concentration, although at very high cell concentrations, such as in a biofilm, saturation kinetics with respect to cell concentration might be observed. Further investigations into the differences between suspended and biofilm kinetics are necessary, as biofilm mediated MICP is a growing focus for applications of MICP (Decho 2010; Cuthbert *et al.* 2012; Cunningham *et al.* 2013).

In urease enzyme kinetic analyses, the enzyme concentration can be compared to whole cell ureolysis by

assuming a constant urease concentration per cell. Krajewska presents a summary of kinetic parameters for ureases, in which the purified urease of *S. pasteurii* is reported to have a maximum activity of 2·5 mol urea (g-enzyme min)$^{-1}$ (Benini *et al.* 1996) and optimal pH of 8·0 (Krajewska 2009). We can assume an intracellular urease concentration of 1% cell dry weight (Bachmeier *et al.* 2002) and the mass of a cell is approx. $3*10^{-13}$ g dry weight (Madigan *et al.* 2003) to estimate a maximum activity per gram urease in whole cells of *S. pasteurii*. These calculations result in an estimated V_{max} of 35·6 mol urea (g-enzyme min)$^{-1}$ for whole cells. This is an order of magnitude higher than the measured V_{max} for the purified enzyme from *S. pasteurii* of 2·5 mol urea (g-enzyme min)$^{-1}$ (Krajewska 2009). This higher affinity inside whole cells may be a result of optimized conditions (pH, co-factors, etc.) for the urease enzyme within the cell compared to the purified enzyme in solution.

The results of the pH dependent kinetic experiments suggest that the rate of ureolysis by *S. pasteurii* in our batch system is not strongly pH dependent within the range of pH 6–9, and only a slight pH dependence is observed in the pH range 5–10. The fitted values of $K_{es,1}$ and $K_{es,2}$ used in Fig. 6 represent the best fit with nonlinear least squares that could be achieved using the commonly used Michaelis–Menten approach (Eqn (7)). The characteristic parabolic shape of the pH dependent model is dictated by the pH dependent term in the denominator of Eqn (7). Optimizing $K_{es,1}$ and $K_{es,2}$ in this equation while maintaining reasonable values for V_{max} and K_m merely succeeds in shifting the maximum pH.

It was determined that this pH dependent rate equation is not a correct form to use in modelling ureolysis by *S. pasteurii* whole cells. Conceptually, these results indicate that urease kinetics in whole cell preparations have a reduced pH dependency compared to free-ureases. The lack of pH dependence of the ureolysis rate in whole cells of *S. pasteurii* suggests that the internal cell pH is regulated which allows for maintenance of the enzyme activity in a wider range of solution pH values.

Ureolysis by whole cells of *S. pasteurii* was not noticeably inhibited by NH_4^+ in the concentration range relevant to ureolytic MICP. Thus, a rate model neglecting the influence of NH_4^+ and pH can be used to predict ureolysis rates at the tested urea and cell concentrations. The results presented here indicate that cell concentration is an important parameter in ureolysis kinetics and must be considered in modelling studies and when controlling MICP technologies by injection of cells or stimulation of cell growth to increase ureolysis rates. Overall, this work provides insight into important parameters for scale-up and technology development of ureolytic MICP applications. Future work will include investigating kinetics of ureolysis in biofilms and the influence of calcium on ureolysis rate, where precipitation on or near the bacterial cells may influence ureolysis.

Acknowledgements

This work was supported by the National Science Foundation's Collaborations in Mathematical Geosciences (CMG) program award no. DMS-0934696 and by the US Department of Energy (DOE) Subsurface Biogeochemical Research (SBR) Program contract no. DE-FG02-09ER64758. Support was provided by Montana State University with a University Scholars Program (USP) undergraduate fellowship for DT. Additional support was provided through the U.S. Department of Energy (DOE) grant numbers DE-FE0004478, DE-FE0009599 and DE-FG02-13ER86571.

Conflict of Interest

No conflict of interest declared.

References

Bachmeier, K.L., Williams, A.E., Warmington, J.R. and Bang, S.S. (2002) Urease activity in microbiologically-induced calcite precipitation. *J Biotechnol* **93**, 171–181.

Barkouki, T.H., Martinez, B.C., Mortensen, B.M., Weathers, T.S., De Jong, J.D., Ginn, T.R., Spycher, N.F., Smith, R.W. *et al.* (2011) Forward and inverse bio-geochemical modeling of microbially induced calcite precipitation in half-meter column experiments. *Transp Porous Media* **90**, 23–39.

Benini, S., Gessa, C. and Ciurli, S. (1996) *Bacillus pasteurii* urease: a heteropolymeric enzyme with a binuclear nickel active site. *Soil Biol Biochem* **28**, 819–821.

Burbank, M.B., Weaver, T.J., Williams, B.C. and Crawford, R.L. (2012) Urease activity of ureolytic bacteria isolated from six soils in which calcite was precipitated by indigenous bacteria. *Geomicrobiol J* **29**, 389–395.

Chahal, N., Rajor, A. and Siddique, R. (2011) Calcium carbonate precipitation by different bacterial strains. *Afr J Biotechnol* **10**, 8359–8372.

Ciurli, S., Marzadori, C., Benini, S., Deiana, S. and Gessa, C. (1996) Urease from the soil bacterium *Bacillus pasteurii*: immobilization on Ca-polygalacturonate. *Soil Biol Biochem* **28**, 811–817.

Connolly, J., Kaufman, M., Rothman, A., Gupta, R., Redden, G., Schuster, M., Colwell, F. and Gerlach, R. (2013) Construction of two ureolytic model organisms for the study of microbially induced calcium carbonate precipitatiom. *J Microbiol Methods* **94**, 290–299.

Cornish-Bowden, A. (2004) *Fundamentals of Enzyme Kinetics*, 3rd edn. London: Portland Press Ltd.

Cunningham, A., Lauchnor, E., Eldring, J., Esposito, R., Mitchell, A., Gerlach, R., Phillips, A., Ebigbo, A. *et al.* (2013) Abandoned well CO_2 leakage mitigation using biologically induced mineralization: current progress and future directions. *Greenhouse Gases Sci Technol* **3**, 40–49.

Cuthbert, M.O., Riley, M.S., Handley-Sidhu, S., Renshaw, J.C., Tobler, D.J., Phoenix, V.R. and Mackay, R. (2012) Controls on the rate of ureolysis and the morphology of carbonate precipitated by *S. pasteurii* biofilms and limits due to bacterial encapsulation. *Ecol Eng* **41**, 32–40.

Cuthbert, M.O., McMillan, L.A., Handley-Sidhu, S., Riley, M.S., Tobler, D.J. and Phoenix, V.R. (2013) A field and modeling study of fractured rock permeability reduction using microbially induced calcite precipitation. *Environ Sci Technol* **47**, 13637–13643.

De Muynck, W., De Belie, N. and Verstraete, W. (2010) Microbial carbonate precipitation in construction materials: a review. *Ecol Eng* **36**, 118–136.

Decho, A.W. (2010) Overview of biopolymer-induced mineralization: what goes on in biofilms? *Ecol Eng* **36**, 137–144.

DeJong, J.T., Mortensen, B.M., Martinez, B.C. and Nelson, D.C. (2010) Bio-mediated soil improvement. *Ecol Eng* **36**, 197–210.

Dupraz, S., Parmentier, M., Menez, B. and Guyot, F. (2009) Experimental and numerical modeling of bacterially induced pH increase and calcite precipitation in saline aquifers. *Chem Geol* **265**, 44–53.

Ebigbo, A., Phillips, A., Gerlach, R., Helmig, R., Cunningham, A.B., Class, H. and Spangler, L.H. (2012) Darcy-scale modeling of microbially induced carbonate mineral precipitation in sand columns. *Water Resour Res* **48**, W07519.

Ferris, F.G., Phoenix, V., Fujita, Y. and Smith, R.W. (2003) Kinetics of calcite precipitation induced by ureolytic bacteria at 10 to 20 degrees C in artificial groundwater. *Geochim Cosmochim Acta* **68**, 1701–1710.

Fidaleo, M. and Lavecchia, R. (2003) Kinetic study of enzymatic urea hydrolysis in the pH range 4-9. *Chem Biochem Eng Q* **17**, 311–318.

Fujita, Y., Taylor, J., Wendt, L., Reed, D. and Smith, R. (2010) Evaluating the potential of native ureolytic microbes to remediate a sr-90 contaminated environment. *Environ Sci Technol* **44**, 7652–7658.

Herigstad, B., Hamilton, M. and Heersink, J. (2001) How to optimize the drop plate method for enumerating bacteria. *J Microbiol Methods* **44**, 121–129.

Jahns, T., Zobel, A., Kleiner, D. and Kaltwasser, H. (1988) Evidence for carrier-mediated, energy-dependent uptake of urea in some bacteria. *Arch Microbiol* **149**, 377–383.

Kantzas, A., Stehmeier, L., Marentette, D.F., Ferris, F.G., Jha, K.N. and Mourits, F.M. (1992) A novel method of sand consolidation through bacteriogenic mineral plugging. In *43rd Annu Tech Meet, Petroleum Soc CIM*. pp. 1–15. Calgary, Alberta.

Krajewska, B. (2009) Ureases I. Functional, catalytic and kinetic properties: a review. *J Mol Catal B Enzym* **59**, 9–21.

Krajewska, B., van Eldik, R. and Brindell, M. (2012) Temperature- and pressure-dependent stopped-flow kinetic studies of jack bean urease. Implications for the catalytic mechanism. *J Biol Inorg Chem* **17**, 1123–1134.

Lauchnor, E., Schultz, L., Bugni, S., Mitchell, A., Cunningham, A. and Gerlach, R. (2013) Bacterially induced calcium carbonate precipitation and strontium coprecipitation in a porous media flow system. *Environ Sci Technol* **47**, 1557–1564.

Madigan, M., Martinko, J. and Parker, J. (2003) *Brock Biology of Microorganisms*, 10th edn. Upper Saddle River, NJ, USA: Pearson Education Inc.

Mahanty, B., Kim, S. and Kim, C. (2014) Biokinetic modeling of ureolysis in *Sporosarcina pasteurii* and its integration into a numerical chemodynamic biocalcification model. *Chem Geol* **383**, 13–25.

Mitchell, A.C., Phillips, A.J., Kaszuba, J.P., Hollis, W.K., Cunningham, A.L.B. and Gerlach, R. (2008) Microbially enhanced carbonate mineralization and the geologic containment of CO_2. *Geochim Cosmochim Acta* **72**, A636.

Mobley, H.L.T. and Hausinger, R.P. (1989) Microbial ureases-Significance, regulation, and molecular characterization. *Microbiol Rev* **53**, 85–108.

Mobley, H.L.T., Island, M.D. and Hausinger, R.P. (1995) Molecular-biology of microbial ureases. *Microbiol Rev* **59**, 451–480.

Moynihan, H.J., Lee, C.K., Clark, W. and Wang, N.H.L. (1989) Urea hydrolysis by immobilized urease in a fixed-bed reactor - analysis and kinetic parameter estimation. *Biotechnol Bioeng* **34**, 951–963.

Okwadha, G.D.O. and Li, J. (2010) Optimum conditions for microbial carbonate precipitation. *Chemosphere* **81**, 1143–1148.

van Paassen, L.A., Ghose, R., van der Linden, T.J.M., van der Star, W.R.L. and van Loosdrecht, M.C.M. (2010) Quantifying biomediated ground improvement by ureolysis: large-scale biogrout experiment. *J Geotech Geoenviron Eng* **136**, 1721–1728.

Parks, S.L. (2009) *Kinetics of calcite precipitation by ureolytic bacteria under aerobic and anaerobic conditions*, thesis Montana State University.

Phillips, A.J., Gerlach, R., Lauchnor, E., Mitchell, A.C., Cunningham, A.B. and Spangler, L. (2013) Engineered applications of ureolytic biomineralization: a review. *Biofouling* **29**, 715–733.

Pinheiro, J.C. and Bates, D.M. (2000) *Mixed-Effects Models in S and S-PLUS, Statistics and Computing Series*. New York, NY: Springer-Verlag.

Pinheiro, J., Bates, D., DebRoy, S., Sarkar, D. and Team, R.D. (2012) nlme: Linear and Nonlinear Mixed Effects Models. R package version 3.1.

Qin, Y.J. and Cabral, J.M.S. (1994) Kinetic-studies of the urease-catalyzed hydrolysis of urea in a buffer-free system. *Appl Biochem Biotechnol* **49**, 217–240.

Stocks-Fischer, S., Galinat, J.K. and Bang, S.S. (1999) Microbiological precipitation of $CaCO_3$. *Soil Biol Biochem* **31**, 1563–1571.

Team, R.C. (2012) *R: A Language and Environment for Statistical Computing*. Vienna, Austria: R Foundation for Statistical Computing.

Tobler, D.J., Cuthbert, M.O., Greswell, R.B., Riley, M.S., Renshaw, J.C., Handley-Sidhu, S. and Phoenix, V.R. (2011) Comparison of rates of ureolysis between *Sporosarcina pasteurii* and an indigenous groundwater community under conditions required to precipitate large volumes of calcite. *Geochim Cosmochim Acta* **75**, 3290–3301.

Zhang, T. and Klapper, I. (2010) Mathematical model of biofilm induced calcite precipitation. *Water Sci Technol* **61**, 2957–2964.

Supporting Information

Additional Supporting Information may be found in the online version of this article:

Table S1. Individual rate data used in kinetic model parameter optimization.

Figure S1. Residuals for nonlinear mixed effects model with random effect for K_m.

Figure S2. Michaelis–Menten model fit to ureolysis rates normalized to CFU, which was calculated from a relationship with OD_{600} (Parks 2009).

Figure S3. Contour plot of the log of the nonlinear least-square cost function.